

TokenMark: A Modality-Agnostic Watermark for Pre-trained Transformers

Hengyuan Xu¹, Liyao Xiang^{*1}, Borui Yang¹, Xingjun Ma², Siheng Chen¹, and Baochun Li³

¹Shanghai Jiao Tong University

²Fudan University

³University of Toronto

Abstract

Watermarking is a critical tool for model ownership verification. However, existing watermarking techniques are often designed for specific data modalities and downstream tasks, without considering the inherent architectural properties of the model. This lack of generality and robustness underscores the need for a more versatile watermarking approach. In this work, we investigate the properties of Transformer models and propose **TokenMark**, a modality-agnostic, robust watermarking system for pre-trained models, leveraging the permutation equivariance property. TokenMark embeds the watermark by fine-tuning the pre-trained model on a set of specifically permuted data samples, resulting in a watermarked model that contains two distinct sets of weights—one for normal functionality and the other for watermark extraction, the latter triggered only by permuted inputs. Extensive experiments on state-of-the-art pre-trained models demonstrate that TokenMark significantly improves the robustness, efficiency, and universality of model watermarking, highlighting its potential as a unified watermarking solution.

1. Introduction

In recent years, deep learning and pre-trained large models have achieved great success. These high-performance backbone models are typically trained using vast amounts of data, expert knowledge, and significant computational resources, making them valuable proprietary assets. However, such assets are constantly at risk of being stolen, redistributed, or exploited by adversaries. In this context, it is crucial for model owners to provide convincing evidence to assert ownership. Watermarking has emerged as a promising tool for the intellectual property (IP) protection of deep learning models [1, 5, 10, 19].

Several challenges remain in watermarking pre-trained

models. As Transformers have become the dominant architecture for pre-training tasks, they have blurred the boundaries between modalities, making existing watermarking schemes for different modalities highly varied. This divergence presents significant obstacles to the scalability, adaptability, and standardization of watermarking practices—without a unified watermarking scheme, no universal standard can be established. Additionally, most mainstream watermarking methods rely on classifiers for classification tasks, which are not well-suited to the modern pretrain-finetune paradigm. Historically, these watermarking methods have been based on backdoors in convolutional neural networks (CNNs). However, recent studies have shown that backdoors in Transformers are more vulnerable to watermark removal attacks [7, 32], suggesting that backdoor-based watermarking schemes may be particularly susceptible to such attacks. Furthermore, the watermarking functions in Transformers remain largely unexplored.

We summarize the challenges of watermarking pre-trained models as follows: **First**, pre-trained models, such as Transformers, often blur the boundaries between modalities and tasks, which contrasts with existing modality-specific, classifier-based watermarking schemes. **Second**, mainstream watermarking methods rely on backdoors, which are not robust in Transformer-based models. These challenges lead to the following question: *Can we design a modality-agnostic, task-independent, and robust watermarking scheme for pre-trained transformers?*

A salient feature of Transformer-based models is their permutation-equivariance [15, 22, 30], meaning that the model’s outputs can be equivalently computed on permuted inputs. Motivated by this property, we explore the possibility of embedding watermarking as a secondary function, independent of the model’s primary task, within the same set of model weights. This secondary function would operate on specifically permuted inputs, rather than the standard ones.

Based on this observation, we propose a novel watermarking scheme, **TokenMark**, which embeds the water-

^{*}Corresponding author: xiangliyao08@sjtu.edu.cn.

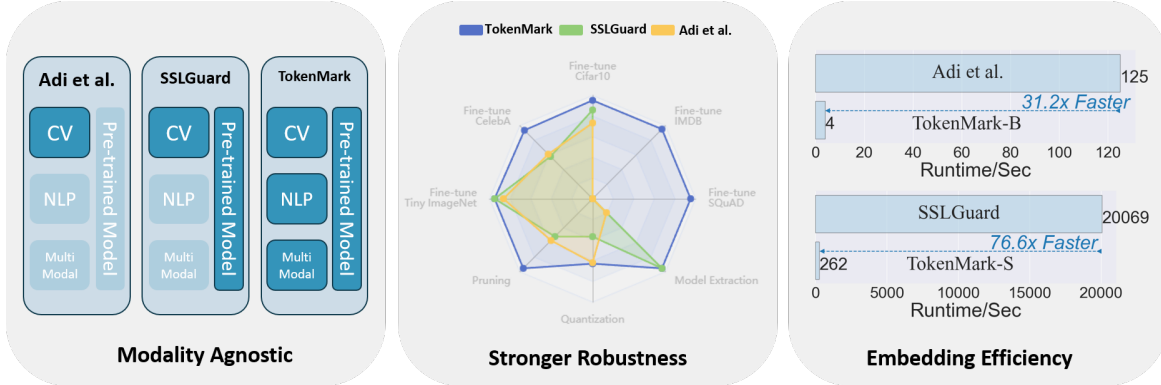


Figure 1. TokenMark is a modality-agnostic, robust, and lightweight watermarking method for pre-trained models. It offers broader applicability and can serve as a universal plugin, replacing the trigger in backdoor-based watermarking systems, thereby enhancing robustness against various watermark removal attacks.

mark as a secondary feature in Transformers, leveraging the permutation equivariance property. Unlike [30], which uses and encrypts only a single set of weights, *TokenMark* constructs two sets of weights within a single model. The normally functioning weights can transform into watermarking weights via simple permutation, triggered by data from *any* dataset of *any* type, permuted by a secret matrix P . Since the watermark embedding is *explicit* with a set of functioning weights—unlike the *implicitly* embedded backdoors—*TokenMark* demonstrates a higher level of generality, robustness, and efficiency (as detailed in Fig. 1) compared to state-of-the-art watermarking schemes.

The highlights of our contributions are as follows: we propose a new watermarking scheme, *TokenMark*, for pre-trained transformers, which is independent of data modality, downstream tasks, and trigger sets. We show that *TokenMark* can serve as a universal plugin for various watermarking systems, significantly enhancing their robustness. We conduct experiments on eight representative pre-trained models performing computer vision (CV), natural language processing (NLP), multimodal tasks, etc. Experimental results confirm the superiority of *TokenMark* over state-of-the-art schemes and highlight its potential to unify different IP protection services into a single solution for model ownership verification.

2. Related Work

IP protection for deep models has become a prominent topic in recent years, especially with the growing use of watermarking schemes. While numerous watermarking methods have been proposed for vision and language models, there is still a scarcity of approaches designed for multi-modal models.

Vision model watermarks often employ backdoor techniques [2, 34] to embed and verify model ownership. A backdoor-based watermark involves attaching a trigger pat-

tern (e.g., a checkerboard pattern) to a small subset of training images and train model f both on the normal dataset and the trigger set D . Done training, the model learns to output a specific (backdoor) class whenever the trigger pattern appears. Various enhancements have been proposed for backdoor-based watermarking systems, including the use of adversarial examples [14], soft nearest-neighbor loss [10], proprietary models [29], and model consistency [11]. In extraction, trigger set D is fed to the suspected model to measure the accuracy of successfully predicting the targeted label. A high watermark rate (WR) defined below indicates the model is watermarked:

$$WR = \frac{|\{x \in D | f(x) = y_t\}|}{|D|}, \quad (1)$$

where y_t is the targeted label.

Language model watermarks differ significantly from vision model watermarks. While embedding-based backdoors are common in vision models, NLP model watermarks are primarily embedding-free. In these cases, detectable patterns are embedded within generated text, which are identifiable by algorithms but not humans [8, 31]. For instance, Kirchenbauer et al. [12] embedded watermarks by selecting a randomized set of “green” tokens before a word is generated, then softly promoting the use of these green tokens during sampling. In large language model-based code generation, Li et al. [17] embedded watermarks by replacing tokens with synonyms. These methods typically alter the model’s outputs to embed the watermark.

Pre-trained model watermarks. The watermarking techniques discussed above are primarily designed for fine-tuned models (such as classifiers or generators) and are not well-suited for pre-trained backbones. In the current AI paradigm, the pre-trained backbone weights represent the core value of a model. However, research on watermarking pre-trained models remains limited. SSLGuard [5] claims to be the first

work to watermark pre-trained backbones. In SSLGuard, the watermark rate is determined by the cosine similarity between the model’s output and a secret key sk :

$$WR = \frac{|x \in D | \text{sim}(sk, G(f(x))) > \epsilon_{wm}|}{|D|}, \quad (2)$$

where G is the trained watermark decoder, ϵ_{wm} is a threshold, and f represents the backbone model. However, this method has limited applicability to other modalities and still relies on an image trigger, with D representing the trigger sample set.

3. Methodology

3.1. Problem Formulation

Given a pre-trained model θ , the defender embeds a watermark to obtain θ_* , ensuring robust extraction to protect against model stealing. The watermark should be effectively and robustly extracted if the model is suspected of being copied by the following types of adversaries.

Black-box adversaries have only API accesses to the victim’s model, along with some reasonable additional knowledge, such as the model structure (e.g., Transformer) and the existence of the watermark. These adversaries are capable of performing extraction attacks [5, 10] to recover the watermark.

White-box adversaries have full access to the model and can freely modify the backbone parameters. We assume that these adversary are capable of performing fine-tuning, pruning, and quantization attacks.

Additionally, we consider an **adaptive attacker**, who is fully aware of our watermarking scheme and designs its attack to overwrite or remove the watermark from the model. While some of these adaptive attackers may be unrealistic in real-world scenarios, they are useful for stress-testing the robustness of the watermarking system and evaluating its ability to defend against more sophisticated adversarial strategies.

3.2. Motivation and Overview

Motivation. TokenMark introduces a novel approach of model watermarking by exploiting the intrinsic permutation symmetry of transformers. The permutation equivariance property [30] of transformers reveals that training on permuted inputs results in a corresponding set of permuted weights, and inference on permuted inputs yields the same output as inference on normal inputs with permuted weights. This property is leveraged for watermark embedding, with permuted inputs serving as backdoors. For watermark extraction, consider $Z \in \mathbb{R}^{n \times d}$ as the input tokens of the transformer and $P \in \mathbb{R}^{d \times d}$ as the permutation matrix. The permuted input ZP can produce the targeted output on θ_* but not on other models. Neither the original inputs Z nor

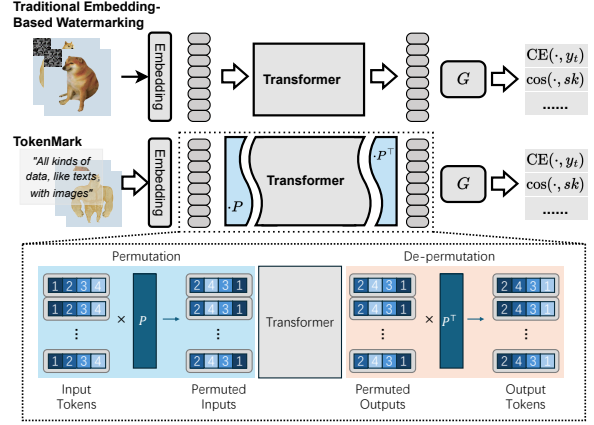


Figure 2. Comparing traditional watermark with TokenMark.

incorrectly permuted inputs ZP' will trigger the watermark on θ_* .

Overview. *TokenMark* operates in two distinct phases: embedding and extraction. Initially, the model owner obtains the original model θ following the standard training procedure. In the embedding phase, θ is fine-tuned on a small ‘embedding set’, which contains arbitrarily selected samples from any dataset. Each sample from this set is permuted by a secret permutation matrix P before being fed into the Transformer backbone. The model’s output is first restored by applying the inverse permutation P^{-1} and then processed by the decoder G to generate the final output. As illustrated in Fig. 2, *TokenMark* separates watermark embedding from input modification: rather than injecting triggers via data poisoning (upper part), it directly encodes watermark into permuted weight subspaces (lower part).

The embedding process results in two sets of parameters within a single model: θ_* and $P(\theta_*)$, where $P(\theta_*)$ represents the permuted weights. While θ_* functions as the original θ , $P(\theta_*)$ is used during watermark extraction. Specifically, $P(\theta)$ includes the permuted version of each weight, denoted with a subscript P :

$$W_P^{(i)} = PW^{(i)}P^{-1}, \quad i = Q, K, V, a, \quad (3)$$

$$W_P^{(1)} = W^{(1)}P^{-1}, W_P^{(2)} = PW^{(2)}, \quad (4)$$

$$b_P = bP^{-1}, \gamma_P = \gamma P^{-1}, \quad (5)$$

where the weights of a Transformer encoder/decoder are $\theta = \{W^{(Q)}, W^{(K)}, W^{(V)}, W^{(a)}, W^{(1)}, W^{(2)}, b, \gamma\}$.

Once embedding is completed, the decoder G and the permutation matrix P are kept secret. During extraction, the permuted extraction set is fed to the model for verification. Unlike backdoor-based watermarking, both the embedding and extraction sets are independent of the trigger set. There are no strict requirements regarding the quantity, content, or form of the data, nor any modification to the input. No-

tably, the extraction set can be completely different from the embedding set.

In summary, the key innovation behind *TokenMark* lies in the exploitation of the permutation equivariance property: the permuted backdoor is embedded with an explicit set of weights, providing a more robust and universal watermark across different modalities. Remarkably, this enables 100% success rate watermark extraction even from heavily tampered models, with just a few embedding samples and steps.

The mechanism by which θ_* and $P(\theta_*)$ co-exist and how $P(\theta_*)$ is embedded, can be explained by the intra-token permutation equivariance property of the Transformer backbone.

3.3. Permutation Equivariance

According to [30], the permutation equivariance property of Transformer-based models holds during both forward and backward propagation. Let $\mathbf{Z} \in \mathbb{R}^{n \times d}$ be the output of the Transformer embedding layer, where n is the number of tokens and d is the dimension of each token. We also refer to \mathbf{Z} as the input tokens to the Transformer backbone F , which consists of a stack of Transformer encoders or decoders.

Theorem 3.1 (Forward equivariance). *The Transformer backbone $F(\cdot)$ is permutation-equivariant during forward propagation, i.e.,*

$$F(\mathbf{Z}\mathbf{P}, \theta)\mathbf{P}^{-1} = F(\mathbf{Z}, P(\theta)), \quad (6)$$

where θ and $P(\theta)$ denote the original and permuted model weights, respectively.

What makes it even more powerful is that the backward permutation equivariance also holds:

Theorem 3.2 (Backward equivariance [30]). *The Transformer backbone $F(\cdot)$ is permutation-equivariant during backward propagation w.r.t. the loss ℓ , i.e.,*

$$\frac{\partial \ell}{\partial \mathbf{W}_P^{(i)}} = \mathbf{P} \frac{\partial \ell}{\partial \mathbf{W}^{(i)}} \mathbf{P}^{-1}, \quad i = Q, K, V, a, \quad (7)$$

$$\frac{\partial \ell}{\partial \mathbf{W}_P^{(1)}} = \frac{\partial \ell}{\partial \mathbf{W}^{(1)}} \mathbf{P}^{-1}, \quad \frac{\partial \ell}{\partial \mathbf{W}_P^{(2)}} = \mathbf{P} \frac{\partial \ell}{\partial \mathbf{W}^{(2)}}, \quad (8)$$

$$\frac{\partial \ell}{\partial b_P} = \frac{\partial \ell}{\partial b} \mathbf{P}^{-1}, \quad \frac{\partial \ell}{\partial \gamma_P} = \frac{\partial \ell}{\partial \gamma} \mathbf{P}^{-1}. \quad (9)$$

Combining Theorem 3.1 and Theorem 3.2, it becomes evident that the Transformer backbone is permutation-equivariant throughout the training by recursion. At the end of a single iteration (one forward pass followed by backward propagation), the resulting model weights θ_* are related to the permuted weights $P(\theta_*)$ as follows:

$$F(\mathbf{Z}\mathbf{P}, \theta_*)\mathbf{P}^{-1} = F(\mathbf{Z}, P(\theta_*)). \quad (10)$$

This implies that if we feed permuted input features $\mathbf{Z}\mathbf{P}$ into F and reverse the permutation on the output features of F , the resulting model weights θ_* would function as $P(\theta_*)$ instead of θ_* . Therefore, by leveraging the forward and backward equivariance properties, we can conclude that the weights of $F(\cdot)$ trained on permuted inputs are equivalent to the permuted weights trained on normal inputs. The permuted set of weights can serve as the second set of weights, distinct from θ .

The specific embedding scheme and watermarking tasks for permutation-based *TokenMark*, based on permutation, can follow any of the approaches used in previous backdoor-based watermarking methods. For example, it could employ the classification approach in Adi et al. [2], or the vector alignment technique in SSLGuard [5]. In Section 3.4 and 3.5, we select two representative watermarking methods from Section 2 to demonstrate how *TokenMark* can enhance their robustness.

3.4. Backdoor Version of *TokenMark*

To illustrate how *TokenMark* enhances conventional backdoor-based watermarking, we introduce a backdoor version of *TokenMark* (denoted as *TokenMark-B*) based on Adi et al. [2], where the watermarking task involves classifying backdoored samples to a target label.

The **embedding** of *TokenMark-B* is similar to the embedding procedure described in Section 2, with one key difference: instead of directly patching the input for the backdoor sample, we permute the input feature (\mathbf{Z}). The permuted inputs are then trained with a cross-entropy loss function as follows:

$$\mathcal{L}_{wm} = \text{CE}(G(F(\mathbf{Z}\mathbf{P}, \theta_*)\mathbf{P}^{-1}), y_t), \quad (11)$$

where y_t is the target label. Any downstream task is trained normally:

$$\mathcal{L}_{DS} = \text{CE}(DS(F(\mathbf{Z}, \theta_*)), y), \quad (12)$$

where y is the ground-truth label. The decoder G is a random mapping, kept secret for the owner.

According to our empirical observation, few-shot or even one-shot learning is typically sufficient for embedding *TokenMark-B*. As a result, we update the pre-trained model using Eq. (11) for only a few epochs to embed the watermark.

The **extraction** of *TokenMark-B* is to decode the target label using samples permuted by \mathbf{P} from the watermarked model. The metric rate (WR) defined in Eq. (1) is used to evaluate extraction performance.

3.5. SSL Version of *TokenMark*

To demonstrate how *TokenMark* enhances watermarking in self-supervised learning (SSL) setting, we introduce a SSL

version of TokenMark (denoted as TokenMark-S), which builds upon SSLGuard [5]. In this setting, the watermarking task is to extract a pre-defined secret vector, denoted as sk , from the model.

The **embedding** process of TokenMark-S focuses on two key objectives: preserving the fidelity of the pre-trained model and ensuring the effective watermark extraction. For fidelity, we aim to keep the original functionality of the pre-trained model without prior knowledge of any downstream task. Similar to SSLGuard, we match the outputs of θ_* to that of θ by minimizing:

$$\mathcal{L}_{DS}(\theta_*) = -\text{sim}(F(\mathbf{Z}, \theta), F(\mathbf{Z}, \theta_*)), \quad (13)$$

where $\text{sim}(\cdot, \cdot)$ denotes the cosine similarity between the two output feature vectors of the model.

For effectiveness, we define a pair of losses, \mathcal{L}_{wm} , which includes a correlation loss on the permuted inputs and an uncorrelated loss on the normal inputs:

$$\mathcal{L}_{corr}(sk, G(F(\mathbf{Z}, P(\theta_*)))) = -\text{sim}(sk, G(F(\mathbf{Z}, P(\theta_*)))) \quad (14)$$

$$\mathcal{L}_{uncorr}(sk, G(F(\mathbf{Z}, \theta_*))) = \text{sim}(sk, G(F(\mathbf{Z}, \theta_*)))^2. \quad (15)$$

Minimizing \mathcal{L}_{uncorr} encourages the cosine similarity to approach zero, ensuring that the two vectors become nearly orthogonal.

The overall embedding loss for the pre-trained model is the sum of the losses for fidelity and effective watermark extraction:

$$\mathcal{L}_B(\theta_*) = \mathcal{L}_{DS}(\theta_*) + \mathcal{L}_{corr}(sk, G(F(\mathbf{Z}, P(\theta_*)))) + \mathcal{L}_{uncorr}(sk, G(F(\mathbf{Z}, \theta_*))). \quad (16)$$

In TokenMark-S, the shadow model used in SSLGuard for robustness is retained. The shadow model θ_s shares the same structure as θ and is trained using the loss function \mathcal{L}_S , which follows the same form as \mathcal{L}_{DS} in Eq. (13) but only replaces θ_* by θ_s . Additionally, the decoder G is trained to extract the secret vector sk from the watermarked model $P(\theta_*)$.

Taking the shadow model into account, the secret vector sk should be extracted from θ_s as well. Moreover, the secret vector should not be decoded from either the unwatermarked model θ or the watermarked model with an incorrect permutation matrix \tilde{P} . Therefore, the loss function for the decoder is defined as:

$$\begin{aligned} \mathcal{L}_G(G) = & \quad (17) \\ & \mathcal{L}_{corr}(sk, G(F(\mathbf{Z}, P(\theta_*)))) + \mathcal{L}_{corr}(sk, G(F(\mathbf{Z}, P(\theta_s)))) \\ & + \mathcal{L}_{uncorr}(sk, G(F(\mathbf{Z}, \tilde{P}(\theta_*)))) + \mathcal{L}_{uncorr}(sk, G(F(\mathbf{Z}, \theta))), \end{aligned}$$

where $F(\mathbf{Z}, \tilde{P}(\theta_*)) = F(\mathbf{Z}\tilde{P}, \theta_*)\tilde{P}^{-1}$ according to the permutation equivariance property. The losses $\mathcal{L}_B, \mathcal{L}_G, \mathcal{L}_S$

are minimized iteratively in the embedding phase. A detailed description of the training procedure can be found in Appendix A.

The **extraction** of TokenMark-S is to feed the pre-trained model with an extraction set permuted by P , restore the output feature by P^{-1} , and feed the restored feature to G to see how the decoded vector aligns with sk . Following SSLGuard, we gauge the metric WR as in Eq. (2) with $\epsilon_{wm} = 0.5$. By our practice, we found that the performance of TokenMark-S is consistently good even when ϵ_{wm} varies in a wide range.

Discussions. Due to space limitation, we move the comparison between TokenMark and the conventional trigger, and the discussion on the secret key space to Appendix C.

4. Experiments

We present the experimental evidence that TokenMark is superior to the trigger-based watermarking scheme in meeting the watermarking requirements. Due to space constraint, we put the detailed setup and partial results in Appendix B.

4.1. Setup

We conduct experiments on eight real-world pre-trained Transformer backbones which are most representative in the field of NLP, CV and multimodal learning, supervised and self-supervised: ViT-timm and ViT-DINOv2 for CV, BERT, GPT-2, and Llama 2 7B for NLP, wav2vec2 for audio, ViT-CLIP for cross-modal, and BLIP-2 for multimodal. In Appendix B, we provide more details about those pre-trained model. Datasets and tasks can be found in Table 3 and more detail can be found in Appendix B, along with detailed embedding configurations and attack configurations.

We first embed the TokenMark and baseline watermarks into the pre-trained models with configurations in Appendix B. Then we evaluate effectiveness, fidelity, efficiency, and robustness of the watermarks.

4.2. Effectiveness, Fidelity and Efficiency

In this section, we verify the efficiency, effectiveness, and fidelity performance of TokenMark.

For **effectiveness**, we measure the watermarking rates of the models watermarked by different methods, as well as the false positive rates of different methods in detecting watermarks on the unwatermarked models. We extract watermarks using three extraction sets. As shown in Table 1 and Table 8, watermarks can be extracted with 100% accuracy from the watermarked models by TokenMark, while shy of 100% extraction accuracy by other methods.

Fidelity of watermarking is evaluated by the gap in the fine-tuning performance between the watermarked model and the original one under the same hyper-parameter setting. The fine-tuning performance is measured by metrics listed in Table 3. Table 2 and Table 9 show that almost all the

Table 1. Effectiveness: WR(%) and False Positive Rate (% in bracket) of different pre-trained CV models. False positive rates are measured on non-watermarked models.

Extraction Set Model	Cifar10			CelebA			ImageNet		
	timm	DINOv2	CLIP	timm	DINOv2	CLIP	timm	DINOv2	CLIP
Adi et al.	99.94 (0.26)	99.93 (4.91)	99.89 (0.89)	89.468 (2.49)	95.19 (2.13)	98.80 (1.85)	98.68 (1.11)	99.16 (5.06)	99.13 (1.98)
TokenMark-B	100.0 (0.00)	100.0 (0.00)	100.0 (0.00)	100.0 (0.00)	100.0 (0.03)	100.0 (0.00)	100.0 (0.00)	100.0 (0.00)	100.0 (0.00)
SSLGuard	100.0 (0.00)	100.0 (0.00)	100.0 (0.00)	100.0 (0.00)	99.79 (11.2)	100.0 (0.21)	100.0 (0.00)	99.68 (0.16)	100.0(0.00)
TokenMark-S	100.0 (0.00)	100.0 (0.08)	100.0 (0.00)	100.0 (0.04)	100.0 (0.01)	100.0 (0.00)	100.0 (0.00)	100.0 (0.04)	100.0 (0.00)

Table 2. Performance of downstream CV tasks on watermarked pre-trained models. Accuracy (%) is used as the metric. In bracket is the accuracy gap compared to the original models (original minus watermarked).

Downstream Model	Cifar10			STL10			CelebA			Tiny-ImageNet		
	timm	DINOv2	CLIP	timm	DINOv2	CLIP	timm	DINOv2	CLIP	timm	DINOv2	CLIP
Adi et al.	98.69(-1.13)	98.67(0.03)	97.48(0.23)	99.05(-1.00)	99.43(-0.65)	97.15(+0.06)	91.23(+0.75)	92.05(-0.77)	92.07(-0.04)	90.87(-0.29)	89.11(0.1)	80.83(-1.32)
TokenMark-B	98.05(-0.49)	98.47(+0.23)	98.13(-0.42)	98.61(-0.56)	98.53(0.75)	97.54(-0.33)	92.01(-0.03)	92.20(-0.92)	92.06(-0.03)	90.89(-0.31)	88.94(+0.34)	79.09(+0.42)
SSLGuard	98.04(-0.35)	99.11(-0.41)	97.48(+0.23)	98.69(-0.70)	99.19(+0.09)	97.44(-0.23)	91.92(+0.06)	92.27(-0.91)	91.96(+0.05)	91.24(-0.66)	89.15(+0.23)	80.57(-1.44)
TokenMark-S	97.47(+0.18)	98.82(-0.12)	97.65(+0.06)	98.02(+0.03)	99.25(+0.03)	97.45(-0.24)	91.82(+0.16)	92.18(+0.10)	92.06(-0.03)	90.40(+0.18)	88.99(+0.29)	79.86(-0.35)

Table 3. Datasets, downstream tasks, fidelity metrics, and fine-tuning epochs.

Datasets	Tasks	Fidelity Metrics	Epochs
CIFAR-10	10-classification	Accuracy	5
STL10	10-classification	Accuracy	5
CelebA	Attributes classification	Accuracy	5
Tiny ImageNet	200-classification	Accuracy	5
IMDB	Binary classification	Accuracy	2
SQuAD	Question answering	Exact Match (EM) F1 score	3
SWAG	Multiple choice	Accuracy	3
WikiText-2	Text generation	Perplexity	1

watermarked models achieve an accuracy (or, exact match and other metrics) within a variance of $\pm 0.5\%$ to the clean accuracy. It confirms that all watermarking methods could well preserve the fidelity in downstream tasks.

To evaluate **efficiency**, we record the runtime of our experiments conducted on a single NVIDIA GeForce RTX 4090 GPU with 24GB memory. As shown on the rightmost side of Fig. 1, while Adi et al. requires 120 seconds (a training epoch) for embedding, TokenMark-B only takes 4 seconds for an effective one-shot embedding. SSLGuard takes even more time, i.e., 5.5 hours (10 training epochs) for embedding, but TokenMark-S only takes 5 minutes (500 steps). Although SSLGuard fine-tunes the model nearly a hundred times more than TokenMark, it still fails to achieve superior robustness, as demonstrated in the following sections.

Table 4. Performance under fine-tuning attack: watermark rates (%) on fine-tuned BERT and GPT-2.

Downstream Model	IMDB		SQuAD		SWAG		WikiText2
	BERT	GPT-2	BERT	GPT-2	BERT	GPT-2	
TokenMark-B	100.0	100.0	100.0	100.0	100.0	100.0	100.0
TokenMark-S	100.0	100.0	100.0	100.0	100.0	100.0	100.0

4.3. Robustness against White-Box Adversaries

A white-box adversary can be encountered in the use case where the model backbone parameters are leaked or made public. We take into consideration the following white-box attacks: fine-tuning, pruning, and quantization, consistent with the previous watermarking literature.

Fine-tuning. We attack the watermarked model by the same fine-tuning configuration as in Appendix B.3. For a more objective view on the robustness against fine-tuning attack, we record the watermark rates on the extraction sets for every fine-tuning epoch.

The WRs under fine-tuning attacks on different CV models are presented in the leftmost three column of Fig. 3 and that on different NLP models in Table 4. Across all settings, TokenMark-B and TokenMark-S achieve almost 100% WRs throughout the fine-tuning process. The CLIP model has the highest robustness for all methods, probably because the pre-trained CLIP aligns texts with images, which are more sensitive to permutation than other models. SSLGuard fails to maintain the watermark performance on CIFAR-10 and CelebA as fine-tuning proceeds, showing its lack of robustness against the attack.

Pruning. It is claimed in [19] that if partial neurons are disabled by pruning, the watermark could be removed from the model. We set the pruning ratio to be r (ranging from 0.1 to 0.5 with a step of 0.1) suggesting r of the neurons in each layer are pruned.

Results are shown in the fourth column of Fig. 3. It is observed that TokenMark-S is highly robust against pruning, and TokenMark-B only fails DINO V2, but still is better than trigger-based baseline. Trigger-based watermarking shows great unstability under pruning. Note that the fall-and-rise pattern of SSLGuard on CLIP is also observed in the contrastive CNN version of SSLGuard in their experiments [5]. Pruning on Llama 2 7B does not affect the WR of TokenMark-B much as shown in Fig. 4, given that the

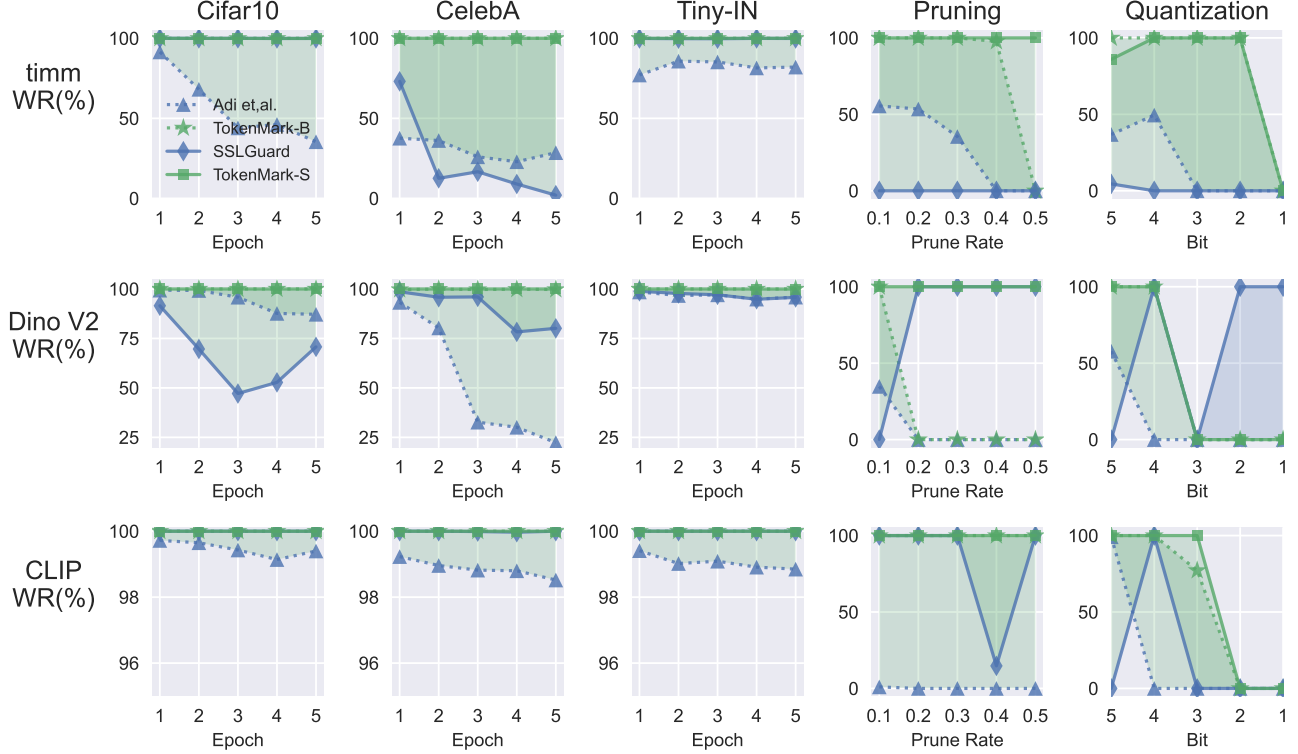


Figure 3. Performance of different watermarking schemes against white-box watermark removal attacks. Regions where TokenMark exceeds the baseline are colored green, otherwise blue. First three columns are fine-tuning attacks using different datasets, and the last two are pruning and quantization attack respectively.

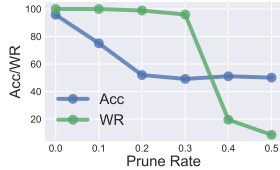


Table 5. Performance of TokenMark-B against quantization attack on Llama. Acc (%) is the accuracy of the downstream task.

Quantization	Acc	WR
Full precision	95.784	100.0
8-bit	96.148	100.0
4-bit	95.996	100.0

Figure 4. Performance of TokenMark-B against pruning attack on Llama. Acc (%) is the accuracy of the downstream task.

task accuracy already decays to random guesses at a higher pruning ratio.

Quantization compresses the model by changing the weights to a lower bit representation, which could be leveraged by the adversary to remove the watermark. We reuse the implementation of [19] for quantization attack. We consider the downstream (fine-tuning) accuracies and the watermark rates under 5-bit to 1-bit quantization. The results are reported in the rightmost column of Fig. 3. TokenMark remains robust against severe quantization, while backdoor-

based watermark, especially SSLGuard, shows an unpredictable rise-and-fall pattern, casting doubt on its robustness against model quantization. For large language model Llama 2 7B, we leverage the LLM quantization tool, bitsandbytes¹, to quantize Llama 2 7B into 4-bit and 8-bit. The watermark remains robust, as shown in Table 5.

4.4. Robustness against Black-Box Adversaries

As reported in [19], watermarks tend to vanish under model extraction attack, since the extracted model might not carry any watermarking functionality. As shown in Table 6, on the extracted models, the WR remains as high as 100%, showing the watermarks are retained after extraction. This can be attributed to the fact that the features of the watermarked models not only carry the main functionality of the pre-trained model but also the watermarking functionality.

4.5. Robustness against Adaptive Adversaries

Finally, we assume an **adaptive adversary**, who has some knowledge of TokenMark-S, including θ_* , sk , $G(\cdot)$, except for P . Leveraging this knowledge, the adversary could

¹<https://github.com/bitsandbytes-foundation/bitsandbytes>

Table 6. Performance under black-box extraction attack: downstream-task Acc (%) and watermark rates (%) on extracted ViTs.

Acc/WR	ViT-timm	ViT-DINOv2	ViT-CLIP
TokenMark-B	95.8/100.0	91.7/100.0	86.7/100.0
TokenMark-S	95.5/100.0	94.6/100.0	89.2/100.0

try to overwrite the existing watermark, or to remove the watermark by reverse-engineering the permutation matrix.

Overwriting. We first assume the adversary tries to embed another watermark with the same strategy, in an attempt to overwrite the original watermark. In TokenMark, the adversary overwrites the watermark by fine-tuning the model with another permutation matrix P' . The overwriting inherits the same configuration with that of the original embedding process, including the hyperparameters and fine-tuning steps. We evaluate the WRs of the original watermark.

Results in Table 7 show that the overwriting fails to eliminate the original watermark. Hence TokenMark is robust to overwriting attacks. We analyze that this is mostly due to the redundant capacity in Transformer-based models to incorporate multiple sets of parameters. We believe multiple permutation matrices could co-exist within one model. The robustness to overwriting attacks can be further extended to the resilience against the ambiguity attack. In resolving the dispute of ownership, the model with only one watermark extracted is the original one belonging to the owner.

Table 7. Performance against overwriting attack: watermark rates (%) on pre-trained models overwritten by CIFAR-10. The embedding and extraction sets are CIFAR-10.

WR	ViT-timm	ViT-DINOv2	ViT-CLIP
TokenMark-B	100.0	100.0	100.0
TokenMark-S	100.0	100.0	100.0

Adaptive Removal. We further assume the adversary tries to remove the watermark by first finding a surrogate permutation matrix P' and then use P' to facilitate a watermark removal attack. To find such a P' , we assume the adversary could perform a brute force attack or gradient-based search attack. The specific methods and formulations can be found in Appendix B.1.

While the brute force strategy in such a huge permutation space (Appendix C.1) is almost impossible, the gradient-based search on ViT-timm could indeed find a permutation matrix P' that achieves 1.0 watermark rate. However, this P' differs from P significantly, with only 0.13% identical elements. As a result of this difference, the removal attempt is not successful: the watermark rate on the de-watermarked model $\hat{\theta}$ w.r.t. P' is reduced to 0.0, but the rate w.r.t. the original P is still almost 1.0. The adversary ends up remov-

ing its own P' but not the original watermark. Additionally, since the real permutation P is also stored at the authority side, it is also impossible for the adversary to cast ambiguity on the model ownership, as P' differs from P and would be immediately identified by the authority as a fake permutation matrix.

5. Limitations and Future Work

While TokenMark is applicable to any attention-based architecture without shifting-window operations, its effectiveness across diverse model configurations and tasks has yet to be thoroughly validated.

TokenMark extends model watermarking from traditional methods to pre-training paradigms, but parameter-efficient fine-tuning (PEFT) techniques like LoRA present new challenges. Adapting such watermarking schemes for the PEFT era requires further investigation.

6. Conclusion

We proposed TokenMark, a watermarking scheme for pre-trained models, which is independent of the data modality, the downstream task, and the trigger set. The design is inspired by the permutation equivariance property of Transformers, and could be adopted to enhance a variety of backdoor-based watermarking systems in terms of robustness and efficiency. Experimental results on a range of pre-trained models and datasets have shown TokenMark’s superiority over the state-of-the-art approaches.

References

- [1] Sahar Abdelnabi and Mario Fritz. Adversarial watermarking transformer: Towards tracing text provenance with data hiding. In *2021 IEEE Symposium on Security and Privacy (SP)*, pages 121–140. IEEE, 2021. 1, 4
- [2] Yossi Adi, Carsten Baum, Moustapha Cisse, Benny Pinkas, and Joseph Keshet. Turning your weakness into a strength: Watermarking deep neural networks by backdooring. In *27th USENIX Security Symposium (USENIX Security 18)*, pages 1615–1631, 2018. 2, 4, 7
- [3] Alexei Baevski, Yuhao Zhou, Abdelrahman Mohamed, and Michael Auli. wav2vec 2.0: A framework for self-supervised learning of speech representations. *Advances in neural information processing systems*, 33:12449–12460, 2020. 2
- [4] Adam Coates, Andrew Ng, and Honglak Lee. An analysis of single-layer networks in unsupervised feature learning. In *Proceedings of the fourteenth international conference on artificial intelligence and statistics*, pages 215–223. JMLR Workshop and Conference Proceedings, 2011. 2
- [5] Tianshuo Cong, Xinlei He, and Yang Zhang. Sslguard: A watermarking scheme for self-supervised learning pre-trained encoders. In *Proceedings of the 2022 ACM SIGSAC Conference on Computer and Communications Security*, pages 579–593, 2022. 1, 2, 3, 4, 5, 6, 7

- [6] Jacob Devlin, Ming-Wei Chang, Kenton Lee, and Kristina Toutanova. Bert: Pre-training of deep bidirectional transformers for language understanding. In *North American Chapter of the Association for Computational Linguistics*, 2019. 2
- [7] Khoa D Doan, Yingjie Lao, Peng Yang, and Ping Li. Defending backdoor attacks on vision transformer via patch processing. In *Proceedings of the AAAI Conference on Artificial Intelligence*, pages 506–515, 2023. 1, 7
- [8] Xuanli He, Qionghai Xu, Yi Zeng, Lingjuan Lyu, Fangzhao Wu, Jiwei Li, and Ruoxi Jia. Cater: Intellectual property protection on text generation apis via conditional watermarks. In *Advances in Neural Information Processing Systems*, pages 5431–5445. Curran Associates, Inc., 2022. 2
- [9] Eric Jang, Shixiang Gu, and Ben Poole. Categorical reparameterization with gumbel-softmax. In *International Conference on Learning Representations*, 2016. 4
- [10] Hengrui Jia, Christopher A Choquette-Choo, Varun Chandrasekaran, and Nicolas Papernot. Entangled watermarks as a defense against model extraction. In *30th USENIX Security Symposium (USENIX Security 21)*, pages 1937–1954, 2021. 1, 2, 3
- [11] Byungjoo Kim, Suyoung Lee, Seanie Lee, Sooel Son, and Sung Ju Hwang. Margin-based neural network watermarking. In *International Conference on Machine Learning*, pages 16696–16711. PMLR, 2023. 2
- [12] John Kirchenbauer, Jonas Geiping, Yuxin Wen, Jonathan Katz, Ian Miers, and Tom Goldstein. A watermark for large language models. In *Proceedings of the 40th International Conference on Machine Learning*, pages 17061–17084. PMLR, 2023. 2
- [13] Alex Krizhevsky, Geoffrey Hinton, et al. Learning multiple layers of features from tiny images. 2009. 2
- [14] Erwan Le Merrer, Patrick Perez, and Gilles Trédan. Adversarial frontier stitching for remote neural network watermarking. *Neural Computing and Applications*, 32:9233–9244, 2020. 2
- [15] Juho Lee, Yoonho Lee, Jungtaek Kim, Adam Kosior, Seungjin Choi, and Yee Whye Teh. Set transformer: A framework for attention-based permutation-invariant neural networks. In *International conference on machine learning*, pages 3744–3753. PMLR, 2019. 1
- [16] Junnan Li, Dongxu Li, Silvio Savarese, and Steven Hoi. Blip-2: Bootstrapping language-image pre-training with frozen image encoders and large language models. In *International conference on machine learning*, pages 19730–19742. PMLR, 2023. 2
- [17] Zongjie Li, Chaozheng Wang, Shuai Wang, and Cuiyun Gao. Protecting intellectual property of large language model-based code generation apis via watermarks. In *Proceedings of the 2023 ACM SIGSAC Conference on Computer and Communications Security*, pages 2336–2350, 2023. 2
- [18] Ziwei Liu, Ping Luo, Xiaogang Wang, and Xiaoou Tang. Deep learning face attributes in the wild. In *Proceedings of the IEEE international conference on computer vision*, pages 3730–3738, 2015. 2
- [19] Nils Lukas, Edward Jiang, Xinda Li, and Florian Kerschbaum. Sok: How robust is image classification deep neural network watermarking? In *2022 IEEE Symposium on Security and Privacy (SP)*, pages 787–804. IEEE, 2022. 1, 6, 7, 3
- [20] Andrew L. Maas, Raymond E. Daly, Peter T. Pham, Dan Huang, Andrew Y. Ng, and Christopher Potts. Learning word vectors for sentiment analysis. In *Proceedings of the 49th Annual Meeting of the Association for Computational Linguistics: Human Language Technologies*, pages 142–150, Portland, Oregon, USA, 2011. Association for Computational Linguistics. 2
- [21] Stephen Merity, Caiming Xiong, James Bradbury, and Richard Socher. Pointer sentinel mixture models. *arXiv preprint arXiv:1609.07843*, 2016. 2
- [22] Muhammad Muzammal Naseer, Kanchana Ranasinghe, Salman H Khan, Munawar Hayat, Fahad Shahbaz Khan, and Ming-Hsuan Yang. Intriguing properties of vision transformers. *Advances in Neural Information Processing Systems*, 34: 23296–23308, 2021. 1
- [23] Maxime Oquab, Timothée Darcet, Théo Moutakanni, Huy Vo, Marc Szafraniec, Vasil Khalidov, Pierre Fernandez, Daniel Haziza, Francisco Massa, Alaaeldin El-Nouby, et al. Dinov2: Learning robust visual features without supervision. *arXiv preprint arXiv:2304.07193*, 2023. 2
- [24] Alec Radford, Jeffrey Wu, Rewon Child, David Luan, Dario Amodei, Ilya Sutskever, et al. Language models are unsupervised multitask learners. *OpenAI blog*, 1(8):9, 2019. 2
- [25] Alec Radford, Jong Wook Kim, Chris Hallacy, Aditya Ramesh, Gabriel Goh, Sandhini Agarwal, Girish Sastry, Amanda Askell, Pamela Mishkin, Jack Clark, et al. Learning transferable visual models from natural language supervision. In *International conference on machine learning*, pages 8748–8763. PMLR, 2021. 2
- [26] Pranav Rajpurkar, Jian Zhang, Konstantin Lopyrev, and Percy Liang. Squad: 100,000+ questions for machine comprehension of text. In *Conference on Empirical Methods in Natural Language Processing*, 2016. 2
- [27] Jingxuan Tan, Nan Zhong, Zhenxing Qian, Xinpeng Zhang, and Sheng Li. Deep neural network watermarking against model extraction attack. In *Proceedings of the 31st ACM International Conference on Multimedia*, pages 1588–1597, 2023. 7
- [28] Alex Wang, Amanpreet Singh, Julian Michael, Felix Hill, Omer Levy, and Samuel R. Bowman. Glue: A multi-task benchmark and analysis platform for natural language understanding. In *Conference on Empirical Methods in Natural Language Processing*, 2018. 2
- [29] Run Wang, Jixing Ren, Boheng Li, Tianyi She, Wenhui Zhang, Liming Fang, Jing Chen, and Lina Wang. Free fine-tuning: A plug-and-play watermarking scheme for deep neural networks. In *Proceedings of the 31st ACM International Conference on Multimedia*, pages 8463–8474, 2023. 2
- [30] Hengyuan Xu, Liyao Xiang, Hangyu Ye, Dixi Yao, Pengzhi Chu, and Baochun Li. Permutation equivariance of transformers and its applications. In *Proceedings of the IEEE/CVF Conference on Computer Vision and Pattern Recognition (CVPR)*, pages 5987–5996, 2024. 1, 2, 3, 4
- [31] KiYoon Yoo, Wonhyuk Ahn, and Nojun Kwak. Advancing beyond identification: Multi-bit watermark for large language models. In *Proceedings of the 2024 Conference of the North American Chapter of the Association for Computational Lin-*

- guistics: Human Language Technologies (Volume 1: Long Papers)*, pages 4031–4055, 2024. [2](#)
- [32] Zenghui Yuan, Pan Zhou, Kai Zou, and Yu Cheng. You are catching my attention: Are vision transformers bad learners under backdoor attacks? In *Proceedings of the IEEE/CVF Conference on Computer Vision and Pattern Recognition*, pages 24605–24615, 2023. [1](#), [3](#), [7](#)
- [33] Rowan Zellers, Yonatan Bisk, Roy Schwartz, and Yejin Choi. Swag: A large-scale adversarial dataset for grounded commonsense inference. In *Conference on Empirical Methods in Natural Language Processing*, 2018. [2](#)
- [34] Jialong Zhang, Zhongshu Gu, Jiyong Jang, Hui Wu, Marc Ph Stoecklin, Heqing Huang, and Ian Molloy. Protecting intellectual property of deep neural networks with watermarking. In *Proceedings of the 2018 on Asia conference on computer and communications security*, pages 159–172, 2018. [2](#)

A. Details of TokenMark-S

Our code is available at <https://anonymous.4open.science/r/TokenMark-D75F/readme.md> for anonymous review.

A.1. The Embedding

The embedding process is a fine-tuning process. Before the embedding, the owner selects a secret permutation matrix P and a secret vector sk . The embedding dataset can be any valid dataset. In each iteration of fine-tuning, a batch of embedding data is sampled to perform three-step updates sequentially: 1) minimizing \mathcal{L}_S over θ_s ; 2) minimizing \mathcal{L}_G over G ; 3) minimizing \mathcal{L}_B over θ_* . After the embedding, the permutation matrix P , the secret vector sk , and the decoder $G(\cdot)$ are kept secret and submitted to the authority, while the watermarked model θ_* or its API access is published. Algorithm 1 provides more detail.

Algorithm 1 Watermark Embedding

Input: 1) The original pre-trained model θ ; 2) randomly-generated (or specifically-designed) permutation matrix P and secret vector sk ; 3) embedding dataset B .

Output: 1) Decoder G ; 2) watermarked model θ_* .

- 1: Initialize θ_* with θ . Initialize θ_s and G randomly.
 - 2: **repeat**
 - 3: Sample a batch of data X from B and get input embeddings $Z = T(X)$
 - 4: Update θ_s w.r.t. \mathcal{L}_S for one step
 - 5: Update G w.r.t. \mathcal{L}_G for one step
 - 6: Update θ_* w.r.t. \mathcal{L}_B for one step
 - 7: **until** Losses converge.
-

A.2. The Extraction

The watermark extraction can be done with white/black-box access to the watermarked model, and API access would suffice for the verification. The extraction set can be any valid dataset, not necessarily the same with the embedding set. The prover only needs to permute its input feature with P and send it to the target model for inference. Applying the forward permutation equivariance in Eq. (6), the inference process is equivalent to inferring Z on $P(\theta_*)$. Then output feature is restored by P^{-1} and is fed into G to decode. The cosine similarity between the decoded vector and the secret vector is calculated. If the similarity is higher than a threshold ϵ_{wm} , the watermark is considered as detected. By calculating the percentage of watermark detected (watermarking rate) in the extraction dataset, the authority can determine whether the pre-trained model belongs to the owner. The detail of the extraction is shown in Algorithm 2.

Algorithm 2 Watermark Extraction

Input: 1) Suspected model θ'_* ; 2) permutation matrix P , secret vector sk , and decoder G ; 3) extraction dataset D .

Output: Watermarking rate WR.

- 1: count = 0, total = 0
 - 2: **repeat**
 - 3: Pick and remove a data record x from D and get input embedding $Z = T(x)$
 - 4: **if** $\text{sim}(G(F(PZ, \theta'_*)P^{-1}), sk) > \epsilon_{wm}$ **then**
 - 5: count += 1
 - 6: **end if**
 - 7: total += 1
 - 8: **until** $D = \emptyset$
 - 9: WR = count / total.
-

B. Experimental Details

B.1. Supplementary Setup

Pre-trained models.

*ViT-timm*² is a Vision Transformer model pre-trained on ImageNet in a supervised manner, provided by PyTorch Image Models(timm). We choose this model as the representative of supervised pre-trained models.

ViT-DINOv2 is a Vision Transformer model pre-trained by DINOv2 [23]. It is pre-trained with self-distillation losses and is one of the most advanced vision encoder nowadays. We choose this model as the representative of self-supervised pre-trained models.

ViT-CLIP is a Vision Transformer model pre-trained as vision encoder in CLIP[25]. It is trained to align the visual representation with the textual representation provided by the text encoder. This model is still the most classic choice when it comes to sentiment analysis on images. We choose this model as the representative of cross-modal pre-trained models.

BERT [6] is a pre-trained model for natural language understanding. We choose this model as the representative of NLP pre-trained encoder models.

GPT-2 [24] is a pre-trained model for natural language generation. We choose this model as the representative of NLP pre-trained auto-regressive models.

BLIP-2 [16] is a pre-trained model for natural language understanding and image-to-text generation. We choose this model to test the performance of TokenMark on advanced multimodal tasks.

*Llama 2*³ is a most representative open source large language model. We choose this model to test the performance of TokenMark on large language models.

Wav2Vec 2.0[3] is a self-supervised speech representation learning model that leverages raw audio data with a transformer architecture, utilizing contrastive learning and quantization to achieve great speech recognition performance with minimal labeled data. We choose this model to test the performance of TokenMark on speech models.

Datasets and downstream tasks.

CIFAR-10 [13] contains 60,000 colored images of size $3 \times 32 \times 32$ from 10 categories, with 6,000 images per class. Adam optimizer is used in fine-tuning with a learning rate of 10^{-4} for ViT-timm and 10^{-5} for the rest.

Tiny-ImageNet is a subset of ImageNet, containing 200 classes, 500 training images, and 50 validation images per class. An Adam optimizer is used in fine-tuning with a learning rate 10^{-5} for all vision models.

STL10 [4] is a subset of ImageNet, containing 10 classes, 5,000 training images and 8,000 test images. Each image is of size $3 \times 96 \times 96$. An Adam optimizer is used in fine-tuning with a learning rate 10^{-4} for ViT-timm and 10^{-5} for the rest.

CelebA [18] is a large-scale face attributes dataset with more than 200K celebrity face images, each with 40 attribute annotations. An Adam optimizer is used in fine-tuning with a learning rate 10^{-4} for ViT-timm and 10^{-5} for the rest.

QNLI [28] is a Natural Language Inference dataset automatically derived from the Stanford Question Answering Dataset v1.1 (SQuAD) and is part of the GLUE benchmark.

IMDB [20] is a dataset for binary sentiment classification. It consists of 50,000 movie reviews from IMDB, with 25,000 for training and 25,000 for testing. An AdamW optimizer with a learning rate 2×10^{-5} is adopted.

SQuAD [26] is a reading comprehension dataset, consisting of questions posed by crowdworkers on a collection of Wikipedia articles, where the answer to every question is a segment of text, or span, from the corresponding reading passage. An AdamW optimizer with a learning rate 2×10^{-5} is adopted.

SWAG [33] is a dataset for grounded commonsense inference, unifying natural language inference and physically grounded reasoning, which contains 113k multiple-choice questions about grounded situations. An AdamW optimizer with a learning rate 5×10^{-5} is adopted for training.

WikiText2 [21] is a language modeling dataset, which is a collection of over 100 million tokens extracted from the set of verified Good and Featured articles on Wikipedia. An AdamW optimizer with a learning rate 5×10^{-5} is adopted for training.

Embedding configurations. We show the embedding detail of our watermarking schemes — TokenMark-B and TokenMark-S, and baselines — Adi et al. [2] and SSLGuard [5] as follows.

Embedding ViTs with Adi et al. [2] and TokenMark-B. We select CIFAR-10 as the embedding set and designate 0 as the target class for triggered samples. A half of the embedding set is triggered for [2] while a set of randomly selected 256 samples is permuted for TokenMark-B. The task head is a randomly initialized linear layer from 768 to 10. The Adam optimizer with a learning rate of 10^{-5} is employed, and the batch size is set to 256. The scheme of Adi et al. is trained for one epoch and TokenMark-B is trained for one step. Extraction sets are test sets of CIFAR-10, CelebA, and ImageNet.

Embedding ViTs with SSLGuard and TokenMark-S. CIFAR-10 is used as the embedding set. The Adam optimizer with learning rate 10^{-5} is adopted with batch size set to 16. SSLGuard is trained for 10 epochs and TokenMark-S is trained for 500 steps. Extraction sets are test sets of CIFAR-10, CelebA, and ImageNet.

²<https://github.com/rwightman/pytorch-image-models>

³<https://www.llama.com/llama2/>

Embedding BERT and GPT with TokenMark. We use 32 records from IMDB for TokenMark-B and 2,400 records from QNLI for TokenMark-S as the default embedding set. The Adam optimizer with learning rate 10^{-5} is employed. TokenMark-B is trained for a single training step and TokenMark-S is trained for 500 steps with batch size 8. Extraction sets are test sets from QNLI, IMDB, and SQuAD.

Embedding LLaMA 2 7B with TokenMark-B. We use 5000 records from IMDB as the embedding set and set 10% of them as permuted samples. An AdamW optimizer with a learning rate of 2×10^{-5} is used. The embedding process is a few-shot full fine-tuning.

Extraction. The watermark threshold ϵ_{wm} is set to 0.5 by default in measuring the watermark rate (WR). Ablation study on ϵ_{wm} shows it has little influence on the watermark rate.

Model architecture and watermark hyperparameters. All the Transformers in this work is base-sized, i.e. 12 layers of 768 dimension Transformer blocks with 12 head and 3072 hidden dimension.

All the downstream heads are a randomly initialized linear layer from 768 to number of classes. The watermarking hyperparameters for TokenMark-S and SSLGuard are as follows: the secret vector sk is a 256-dimensional vector randomly generated from a standard normal distribution. The watermark decoder G is a 2-layer Multi-Layer Perceptron (MLP) with a hidden layer of size 256 and ReLU activation. The first token of the output of the transformer backbone is used for decoding the watermark. Additionally, dropout mechanism is applied on the output of each Transformer block in the embedding process to enhance the robustness of watermarking.

Trigger pattern for Adi et al. is a pure white patch of size 16×16 at the top-left corner of the 224×224 image, which is designed according to [32]. And the trigger pattern for SSLGuard is from its original work [5].

Attack configurations. For the black-box extraction attack, we adopt the same extraction attack as in [5], using CelebA as the adversary’s extracting dataset, to evaluate the robustness of TokenMark. The extraction attacker aligns the feature of its extracted model with that of the watermarked model, by minimizing the cosine similarity between the model outputs. SGD optimizers with learning rate 10^{-4} for ViT-timm and 10^{-5} for ViT-DINOv2 and ViT-CLIP are applied for optimization.

(White-box) Fine-tuning attack. To make the scene resemble an actual attack, we use the setup in Table 3 where the fine-tuning takes 5 epochs ensuring the downstream tasks are truly optimized. For a more objective view on the robustness against fine-tuning attack, we record the watermark rates on the extraction sets for every fine-tuning epoch.

(White-box) Pruning. It is claimed in [19] that if partial neurons are disabled by pruning, the watermark could be removed from the model. A pruning ratio r is set, and r of the neurons in each layer are pruned. We set r ranging from 0.1 to 0.5 with a step of 0.1. By pruning we set the smallest r of the neurons in the backbone to zero.

(White-box) Quantization compresses the model by changing the weights to a lower bit representation, which could be leveraged by the adversary to remove the watermark. We reuse the implementation of [19] for quantization attack. We consider the downstream (fine-tuning) accuracies and the watermark rates under 5-bit to 1-bit quantization. We did not truly quantize the model to like fp16 or int4, but we simulate the quantization by changing the weights to the nearest quantized value. Like in 5-bit quantization, there are only 32 possible values for the weights.

(Black-box) Model extraction attack tend to vanish under model extraction attack, since the extracted model might not carry any watermarking functionality. We adopt the same extraction attack as in [5], using CelebA as the adversary’s extracting dataset, to evaluate the robustness of TokenMark. The extraction attacker aligns the feature of its extracted model with that of the watermarked model, by minimizing the cosine similarity between the model outputs. SGD optimizers with learning rate 10^{-4} for ViT-timm and 10^{-5} for ViT-DINOv2 and ViT-CLIP are applied for optimization.

(Black-box) Model distillation is a widely adopted technique in contemporary deep learning practices. It involves training a smaller, more compact model to replicate the behavior of a larger, more complex model. In this context, we investigate whether the watermark embedded in the teacher model can be inherently transferred to the distilled student model. To explore this, we employ the same distillation loss function as used in the extraction attack. Specifically, the teacher model is a pre-trained ViT-timm, while the student model is a randomly initialized Vision Transformer (ViT) with the same embedding dimension (768) but half the number of layers (6). The student model is trained over 300 epochs with a learning rate of 10^{-4} .

(Adaptive attack) Brute force by random search. We allow the attacker to randomly generate a batch of \mathbf{P}' s as the permutation matrices, in an effort to extract the watermark from θ_* . If the adversary obtains a WR greater than 0.5 on a very small dataset, it then verifies that permutation on the entire extraction set. If the WR is still greater than 0.5, we consider the random search successful.

(Adaptive attack) Gradient-based search and adaptive removal. We further consider an adversary who first finds a surrogate permutation matrix \mathbf{P}' via gradient-based optimization, and then uses \mathbf{P}' to instantiate a watermark removal attack. The adversary first initializes and obtains a matrix \mathbf{P}' by minimizing

$$\mathcal{L}_a = -\cos(G(F(\mathbf{Z}, \mathbf{P}'(\theta_*))), sk) + \alpha \|\mathbf{I} - \sigma(\mathbf{P}'^\top) \sigma(\mathbf{P}')\|_2^2,$$

Table 8. Effectiveness: WR(%) of different pre-trained NLP models. The notations are the same with Table 1.

Extraction Set	QNLI		IMDB		SQuAD	
Model	BERT	GPT-2	BERT	GPT-2	BERT	GPT-2
TokenMark-B	100.0 (0.00)	100.0 (0.00)	100.0 (0.00)	100.0 (0.04)	100.0 (0.00)	100.0 (0.07)
TokenMark-S	100.0 (0.00)	100.0 (0.00)	100.0 (0.00)	100.0 (0.00)	100.0 (0.00)	100.0 (0.00)

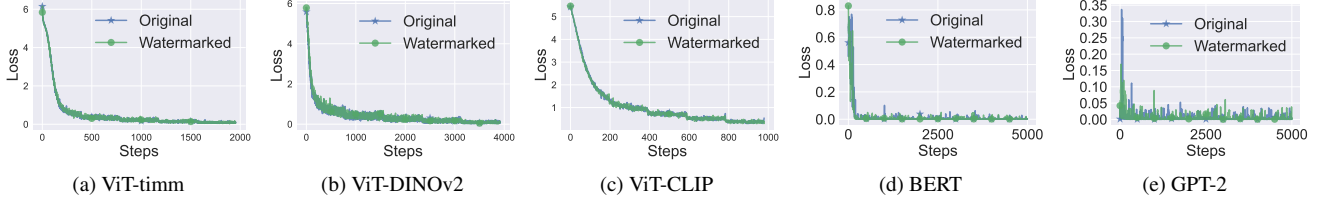


Figure 5. Loss curves of fine-tuning with original backbone and watermarked backbone. CV models are fine-tuned on Tiny ImageNet and NLP models are fine-tuned on IMDB.

where $\sigma(\cdot)$ denotes the Softmax activation function and $\alpha = 0.1$ is a hyper-parameter. We ensure each row of \mathbf{P}' to be a one-hot vector via Gumbel-Softmax sampling [9], which is a commonly used trick for sampling discrete one-hot vectors while allowing for gradient back-propagation [1]. We run the optimization on CIFAR-10 dataset for 3 epochs, and convert the obtained \mathbf{P}' into a 0-1 matrix by setting the largest value of each row as 1 and the rest as 0. Note that the obtained \mathbf{P}' is not necessarily a permutation matrix, but thanks to the L_2 regularization in \mathcal{L}_a , it is *almost* one, with only a few duplicated or missing rows. The adversary could easily make \mathbf{P}' a valid permutation matrix by randomly replacing duplicated rows with missing elements at a negligible loss.

The adversary could then use its obtained \mathbf{P}' to facilitate a watermark removal attack, by training a de-watermarked model parametrized by $\hat{\theta}$ to minimize the loss

$$\mathcal{L}_{rm} = -\text{sim}(F(\mathbf{Z}, \hat{\theta}), F(\mathbf{Z}, \theta_*)) + \text{sim}^2(sk, G(F(\mathbf{Z}, \mathbf{P}'(\hat{\theta})))),$$

where $\hat{\theta}$ is initialized from the watermarked model θ_* .

Setup of Fig. 1. There is no additional experiments conducted for Fig. 1. The middle subfigure shows the averaged results on robustness. The fine-tuning results are averaged over the WRs of three testing models, and the pruning and quantization results are averaged over all the pruning ratios/quantization bits of three testing models, respectively. The rightmost subfigure is the recorded running time on ViT-timm.

B.2. Results on Effectiveness and Efficiency

In this section, we verify the effectiveness, integrity, and efficiency performance of TokenMark.

For **effectiveness**, we measure the watermarking rates of the models watermarked by different methods, as well as the false positive rates of different methods in detecting watermarks on the unwatermarked models. We extract watermarks using three extraction sets. Note that the original implementation of SSLGuard uses the same dataset for both embedding and extraction, but TokenMark does not have such a requirement.

Results. As shown in Table 1 and Table 8, watermarks can be extracted with 100% accuracy from the watermarked models by TokenMark, while shy of 100% extraction accuracy by other methods. The high WR may be attributed to the vulnerability of Transformer models to backdoors, despite their forms. Notably, TokenMark can extract watermarks from out-of-distribution data with 100% accuracy, e.g., in cases where the extraction set is not CIFAR-10. The WR shy of 100% in these cases for Adi et al. and SSLGuard indicates these watermarking methods have some transferability to unseen extraction sets, but cannot guarantee 100% extraction. Meanwhile, the false positive rates are almost all zeros for TokenMark but not for Adi et al. and SSLGuard, suggesting the baseline methods may wrongly detect watermarks from unwatermarked models.

To evaluate **efficiency**, we record the runtime of our experiments conducted on a single NVIDIA GeForce RTX 4090 GPU with 24GB memory. As shown on the rightmost side of Fig. 1, while Adi et al. requires 120 seconds (a training epoch) for embedding, TokenMark-B only takes 4 seconds for an effective one-shot embedding. SSLGuard takes even more time, i.e., 5.5 hours (10 training epochs) for embedding, but TokenMark-S only takes 5 minutes (500 steps).

The results show that TokenMark satisfies the basic effectiveness requirement of watermarking, and is lightweight to run.

Table 9. Performance of downstream NLP tasks on watermarked pre-trained models. Metrics of IMDB and SQuAD are accuracy (%). The metric of SWAG is Exact Match (EM) (%) while that of WikiText2 is perplexity. The former three metrics are the higher the better, while the latter is the lower the better. In bracket is the performance gap compared to the original models (original minus watermarked).

Downstream Model	IMDB BERT	GPT-2	SQuAD BERT	GPT-2	SWAG BERT	WikiText2 GPT-2
TokenMark-B	94.00(-0.13)	93.85(-0.37)	80.63(-0.81)	67.71(-0.06)	80.47(-0.15)	30.20(+0.00)
TokenMark-S	93.95(-0.08)	93.58(-0.10)	79.89(-0.07)	67.89(-0.24)	80.10(+0.22)	30.14(-0.06)

Table 10. Robustness against distillation: WR(%) of the distilled models.

Teacher	Student	Acc (%)	WR
12-layer ViT-timm	6-layer ViT	87	1.0
None	6-layer ViT	72	-

B.3. Results on Watermark Fidelity

The fidelity of watermarking is evaluated by the gap in the fine-tuning performance between the watermarked model and the original one under the same hyper-parameter setting. The fine-tuning performance is measured by metrics listed in Table 3. The three vision models are fine-tuned on CIFAR-10, STL10, CelebA and Tiny ImageNet, and the two NLP models are fine-tuned on IMDB, SQuAD, SWAG (for BERT), and WikiText2 (for GPT), respectively.

Results show that almost all the watermarked models achieve an accuracy (or, exact match and other metrics) within a variance of $\pm 0.5\%$ to the clean accuracy. It confirms that all watermarking methods could well preserve the fidelity in downstream tasks. The fine-tuning loss curves of the original model and the model watermarked by TokenMark-S are presented in Fig. 5. The results demonstrate that the watermark almost has no impact on the fine-tuning process.

The supplementary results are shown in Table 2 (CV) and Table 9 (NLP). Metrics for CV tasks, IMDB and SQuAD are accuracy. The metric for SWAG is exact match, and that for WikiText2 is perplexity. The perplexity is the lower the better, while all other metrics are the higher the better. Detailed fine-tuning hyperparameters are provided in Sec. B.1.

B.4. Results on Robustness of BLIP-2 and Wav2Vec 2.0

We further assess the robustness of TokenMark across diverse real - world multimodal and audio tasks. For the multimodal task of image captioning, we employ BLIP - 2; for the audio task of speech recognition, we utilize wav2vec2. The conclusions drawn from these experiments are consistent with those of our main experiments. Specifically, we fine - tune a watermarked BLIP - 2 on a customized sports image captioning dataset⁴. The loss on the test set is 0.115, which is remarkably close to the loss of the original model (0.119), and the Watermark Recall (WR) stands at 100%. Similarly, when we fine - tune a watermarked wav2vec2 on the SUPERB keyword spotting dataset⁵, the test set accuracy reaches 98.35%, close to the original model’s accuracy of 98.15%, with a WR of 100% as well.

B.5. Results on Robustness against Distillation

We evaluate the robustness of *TokenMark* against model distillation by training a 6-layer Vision Transformer (ViT) under the guidance of a 12-layer ViT-timm teacher model. To provide a comprehensive comparison, we also train the student model from scratch without distillation. The results demonstrate that the guidance from the teacher model significantly enhances the student model’s accuracy, improving it from 72% to 87%. Notably, *TokenMark* is fully preserved in the distilled model, achieving a 100% inheritance rate, as detailed in Table 10.

B.6. Study of Hyperparameters

We study how the change of some hyperparameters affects TokenMark’s performance.

Watermark threshold ϵ_{wm} is set to 0.5 by default in measuring WR. Here we vary the value from 0.050 to 0.999 in extracting the watermark from ViT-timm, ViT-DINOv2 by CIFAR-10, both using the watermarked model ($P(\theta_*)$), the unwatermarked model ($P(\theta)$) and the incorrectly extracted one ($\tilde{P}(\theta_*)$) in TokenMark-S. As shown in Fig. 6, for ViT-timm, the threshold does not affect WRs where $0.30 < \epsilon_{wm} < 0.997$. The safe region for DINOv2 is $\epsilon_{wm} < 0.995$. A too-low threshold incurs false positives on both unwatermarked and incorrectly decoded model while a too high value leads to false

⁴<https://huggingface.co/datasets/ybelkada/football-dataset>

⁵<https://huggingface.co/superb/wav2vec2-base-superb-ks>

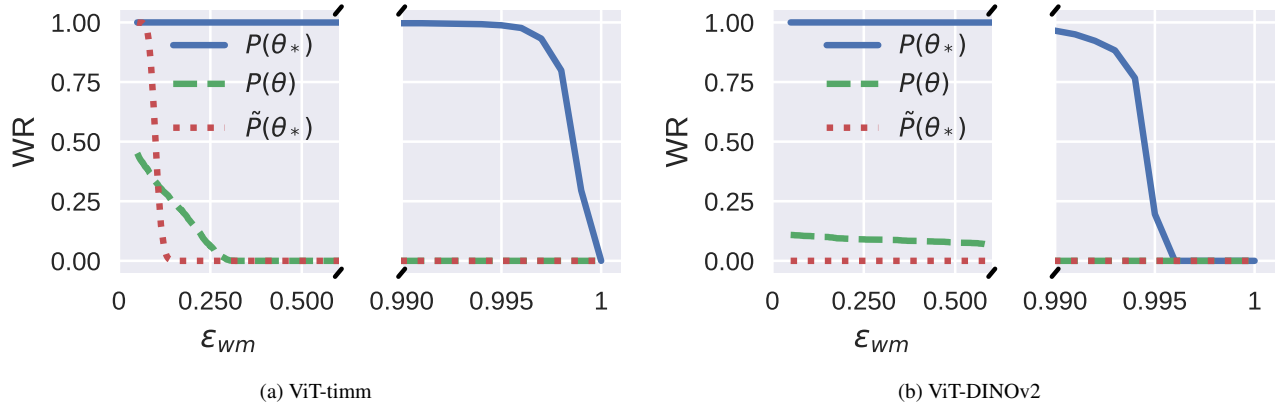


Figure 6. Watermark rates with different ϵ_{wm} s in TokenMark-S. $P(\theta_*)$, $P(\theta)$, $\tilde{P}(\theta_*)$ represent the watermarked model, unwatermarked model, and the incorrectly decoded model, respectively.

negatives. Overall, most decoded vectors either have a very high similarity, or almost zero similarity to the secret vector. Hence TokenMark is quite robust to the change in ϵ_{wm} .

Size of extraction set also has little influence on the watermark rate. To observe its influence, we specifically select watermark extraction from ViT-timm in TokenMark-S with $\epsilon_{wm} = 0.998$ at which the WR is shy of 1.00. In that case, we vary the CIFAR-10 extraction set size from 10 to 10000. The change of WR is mostly observed to follow the law of large numbers and it converges to 0.52.

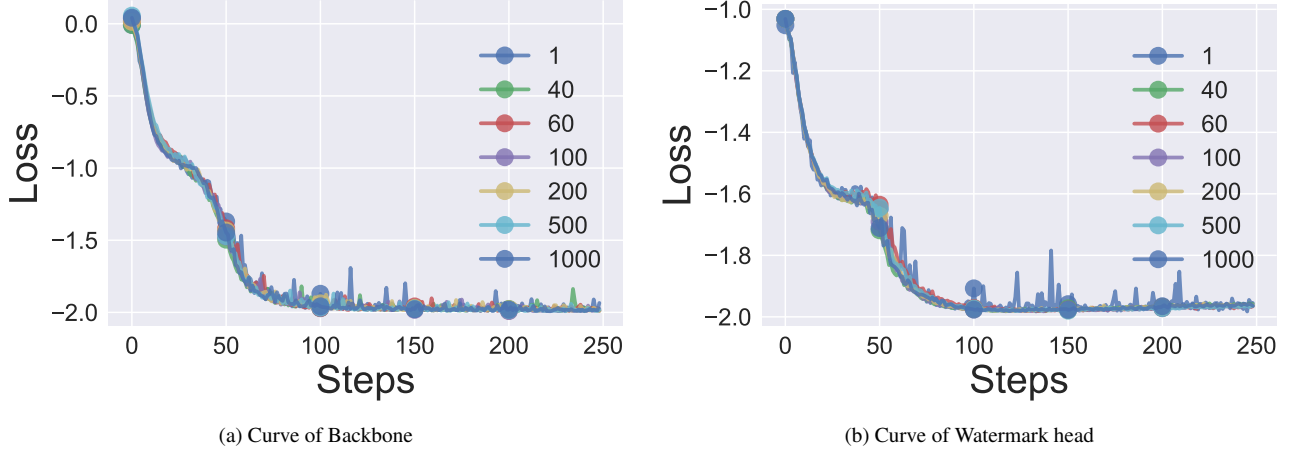


Figure 7. Loss curves of embedding TokenMark-S watermark with different embedding set sizes.

Size of embedding set. We have tried embedding TokenMark-S watermarks using fewer CIFAR-10 images (1000, 500, 200, 100, 60, 40 and 1) and more training epochs (5, 10, 25, 50, 85, 125, and 250) accordingly. The embedding loss curves are not much different from one another, as shown in Fig. 7. Its effectiveness (a) and fidelity performance (b) are as good as the default setting, but the robustness decays given too few embedding samples. Taking single-image embedding as an example, its watermark survived fine-tuning on CIFAR-10 and STL10, but not CelebA, nor pruning attack ($r > 0.2$). A possible explanation is that too few data records may induce memorization of outlier examples, and in this situation, the watermark may degenerate into a data-driven one violating the principle of TokenMark.

C. Discussions

C.1. Discussion on Permutation Watermarking

While permutation in *TokenMark* can be considered a new type of backdoor trigger, it is essentially different from the conventional trigger.

First of all, the traditional trigger-based watermarking schemes are data-driven, relying heavily on the trigger pattern and embedding set distribution. This brings two major defects for previous watermarking schemes: 1) The watermarking schemes weaken on Transformer-based models as these models are more vulnerable to backdoors [7, 32] than CNNs, leading to easy removal of the backdoor. 2) According to [27], the extracted model may not maintain the watermark particularly when the extraction data has a different distribution from the embedding data. In contrast, *TokenMark* is structure-driven, thereby eliminating all the drawbacks of the conventional trigger. Since the permutation is associated with the model itself, rather than any dataset or any downstream task, our watermarking scheme is universal across different modalities.

Second, it may be considered viable to reconstruct permutation by reverse engineering, but the hardness of permutation recovery is at least comparable to trigger reconstruction, if not harder. Let’s assume the hidden dimension of the model is at the same order with the number of pixels of an image trigger, e.g., $d = 768$ for a base-size ViT. The number of possible trigger patterns is 256^d which is orders of magnitude less than the number of possible permutations $d!$. Hence the random search attack to reverse the permutation is at least as hard as reconstructing the trigger pattern. In fact, the permutation reversing is symmetric to the trigger reconstruction as the attacker works on the model weights and inputs, respectively. The former problem is more difficult to tackle as the permutation space is discrete, while the trigger space can be continuous over which is easier to optimize by gradient-based methods.

For a deeper analysis on the permutation space, we give the following example. Taking the base-size Transformer as an example, its token dimension $d = 768$ and thus the permutation matrix is of size $\mathbb{R}^{768 \times 768}$. Constrained by multi-head operation, the permutation is limited inside each head, but not across heads, which leads to a total of $12! \times 64! \approx 6.1 \times 10^{97}$ possible permutations (as we only consider column shuffling). It is almost impossible for an adversary to launch a brute-force attack to derive the permutation order. Further, any proprietary or commercial pre-trained model could easily have much higher dimensions than the base size. The larger the model, the more secure the watermark.

TokenMark may seem vulnerable in LLM given that an adversary with the embedding vocabulary can search the permutation matrix by brute-force. However, the adoption of the absolute position embedding to the input tokens prevents such an attack due to unknown embedding weights. Although an additional absolute position embedding may have no effect on the model’s performance, it still needs full fine-tuning to adapt to this modification, causing inconvenience to directly adapt *TokenMark* to LLM.

C.2. Discussion on Robustness Results

We now provide a deeper analysis on the reason behind *TokenMark*’s robustness. First, as has been stated in Sec. ??, *TokenMark*’s watermark is structure-driven — embedding the watermark by the permutation order of model weights, which are barely associated with a particular dataset. On the other hand, trigger-based schemes, represented by Adi et al.[2] and SSLGuard[5], are data-driven — relying heavily on the trigger patterns. Hence the model weights are tied to the trigger set. Once the model parameters are pruned or fine-tuned, some ‘key’ neurons may be modified and thus the triggering path disappears. However, such changes hardly affect the permutation order of the weights, thus preserving *TokenMark*’s watermarking functionality. Second, Transformer-based models are more vulnerable to backdoors [7, 32], meaning that it is easier to implant or remove a backdoor for Transformer models. Transformers are thereby less robust in trigger-based watermarking, compared to the ResNet models used in the original SSLGuard. Third, in face of black-box model extraction attack, the trigger-based scheme hinges upon the trigger data distribution which could be quite different from the extracting data used by the attacker, and hence the extracted model easily removes the watermark without affecting the major functionality of the model. In contrast, the watermark of *TokenMark* is closely tied up with the weights, and the extracted model would largely preserve the watermark as an inherent feature.

We provide an intuition on why it is hard for the adversary to invert \mathbf{P} . Assuming the backbone F and decoder G only contain linear layers, the adversary essentially solves the following equations to obtain \mathbf{P}' :

$$G \cdot F(\mathbf{Z}, \mathbf{P}'(\theta_*)) = sk.$$

The unknowns of the equations are collectively represented by \mathbf{P}' which is orders of magnitude larger than the dimension of sk (256 in *TokenMark*-S and 10 in *TokenMark*-B). Hence the equations would have many solutions, and it is almost impossible for the adversary to identify the \mathbf{P} .